Orbital Dynamics of Eccentric Compact Binaries

Alexandre Le Tiec

Laboratoire Univers et Théories
Observatoire de Paris / CNRS

Collaborators: S. Akcay, L. Barack, N. Sago, N. Warburton

Phys. Rev. D **91** 124014 (2015), arXiv:1503.01374 [gr-qc]
Phys. Rev. D **92** 084021 (2015), arXiv:1506.05648 [gr-qc]

Outline

① Gravitational wave source modelling

② Averaged redshift for eccentric orbits

③ First law of mechanics and applications

Outline

① Gravitational wave source modelling

② Averaged redshift for eccentric orbits

③ First law of mechanics and applications

Source modelling for compact binaries

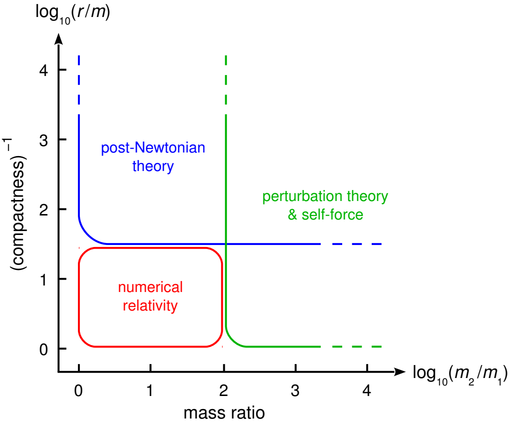

Source modelling for compact binaries

$$q \equiv \frac{m_1}{m_2} \ll 1$$

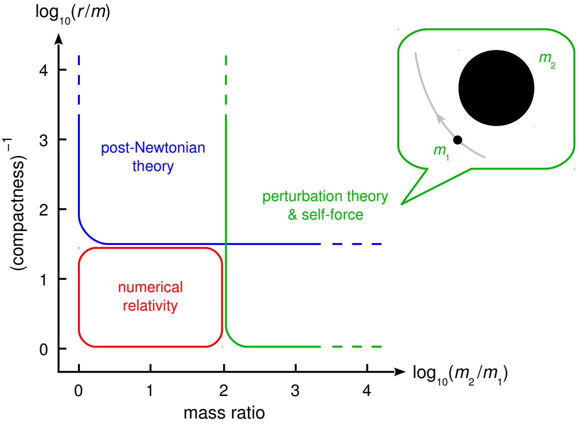

Source modelling for compact binaries

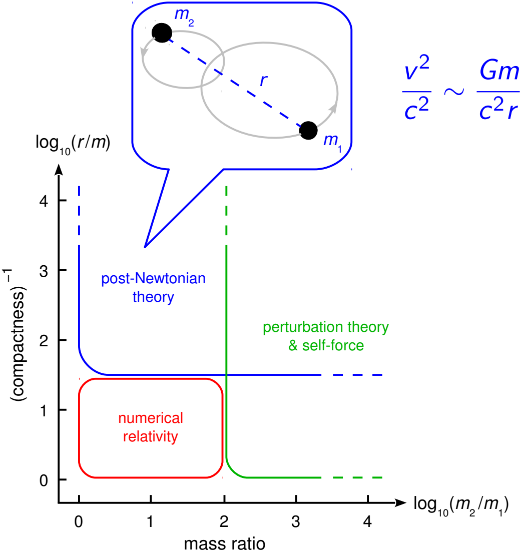

$$\frac{v^2}{c^2} \sim \frac{Gm}{c^2 r} \ll 1$$

Source modelling for compact binaries

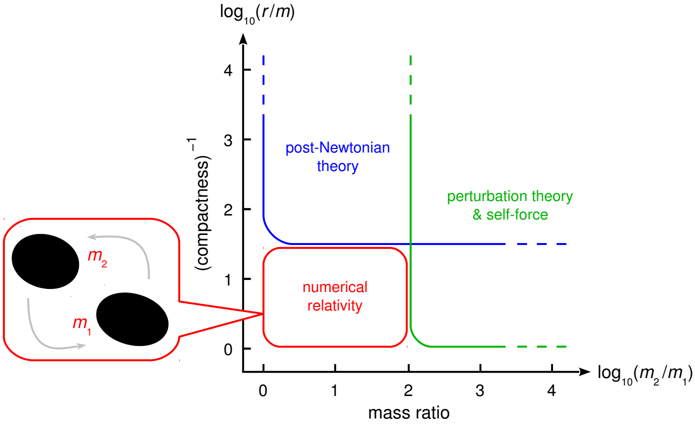

Source modelling for compact binaries

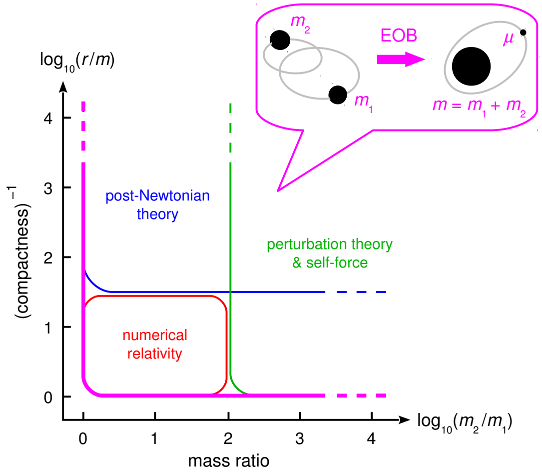

Comparing the predictions from these methods

Why?

- Independent checks of long and complicated calculations
- Identify domains of validity of approximation schemes
- Extract information inaccessible to other methods
- Develop a universal model for compact binaries

Comparing the predictions from these methods

Why?

- Independent checks of long and complicated calculations
- Identify domains of validity of approximation schemes
- Extract information inaccessible to other methods
- Develop a universal model for compact binaries

How?

✘ Use the same coordinate system in all calculations

✔ Using coordinate-invariant relationships

Comparing the predictions from these methods

Why?

- Independent checks of long and complicated calculations
- Identify domains of validity of approximation schemes
- Extract information inaccessible to other methods
- Develop a universal model for compact binaries

How?

✘ Use the same coordinate system in all calculations

✔ Using coordinate-invariant relationships

What?

- Gravitational waveforms at future null infinity
- Conservative effects on the **orbital dynamics**

Comparing the predictions from these methods

Paper	Year	Methods	Observable	Orbit	Spin
Detweiler	2008	SF/PN	redshift observable		
Blanchet et al.	2010	SF/PN	redshift observable		
Damour	2010	SF/EOB	ISCO frequency		
Mroué et al.	2010	NR/PN	periastron advance		
Barack et al.	2010	SF/EOB	periastron advance		
Favata	2011	SF/PN/EOB	ISCO frequency		
Le Tiec et al.	2011	NR/SF/PN/EOB	periastron advance		
Damour et al.	2012	NR/EOB	binding energy		
Le Tiec et al.	2012	NR/SF/PN/EOB	binding energy		
Akcay et al.	2012	SF/EOB	redshift observable		
Hinderer et al.	2013	NR/EOB	periastron advance		✓
Le Tiec et al.	2013	NR/SF/PN	periastron advance		✓
Damour et al.	2014	NR/PN/EOB	scattering angle	hyperbolic	
Bini, Damour; Shah et al.; Blanchet et al	2014	SF/PN	redshift observable		
Dolan et al.; Bini, Damour	2014	SF/PN	precession angle		✓
Isoyama et al.	2014	SF/PN/EOB	ISCO frequency		✓
Akcay et al.	2015	SF/PN	averaged redshift	eccentric	

Comparing the predictions from these methods

Paper	Year	Methods	Observable	Orbit	Spin
Detweiler	2008	SF/PN	redshift observable		
Blanchet et al.	2010	SF/PN	redshift observable		
Damour	2010	SF/EOB	ISCO frequency		
Mroué et al.	2010	NR/PN	periastron advance		
Barack et al.	2010	SF/EOB	periastron advance		
Favata	2011	SF/PN/EOB	ISCO frequency		
Le Tiec et al.	2011	NR/SF/PN/EOB	periastron advance		
Damour et al.	2012	NR/EOB	binding energy		
Le Tiec et al.	2012	NR/SF/PN/EOB	binding energy		
Akcay et al.	2012	SF/EOB	redshift observable		
Hinderer et al.	2013	NR/EOB	periastron advance		✓
Le Tiec et al.	2013	NR/SF/PN	periastron advance		✓
Damour et al.	2014	NR/PN/EOB	scattering angle	hyperbolic	
Bini, Damour; Shah et al.; Blanchet et al	2014	SF/PN	redshift observable		
Dolan et al.; Bini, Damour	2014	SF/PN	precession angle		✓
Isoyama et al.	2014	SF/PN/EOB	ISCO frequency		✓
Akcay et al.	**2015**	**SF/PN**	**averaged redshift**	**eccentric**	

Outline

Post-Newtonian expansions and black hole perturbations

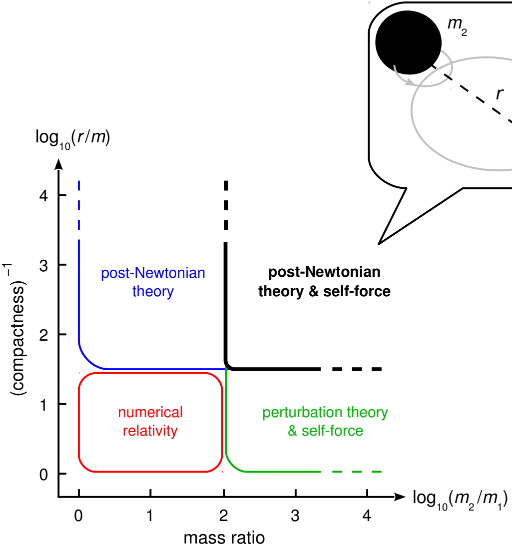

Averaged redshift for eccentric orbits

- Generic eccentric orbit parameterized by the two invariant frequencies

$$n = \frac{2\pi}{P}\,, \quad \omega = \frac{\Phi}{P}$$

- Time average of $z = \mathrm{d}\tau/\mathrm{d}t$ over one radial period [Barack & Sago 2010]

$$\langle z \rangle \equiv \frac{1}{P}\int_0^P z(t)\,\mathrm{d}t = \frac{T}{P}$$

- Coordinate-invariant relation $\langle z \rangle(n,\omega)$ is well defined in GSF and PN frameworks

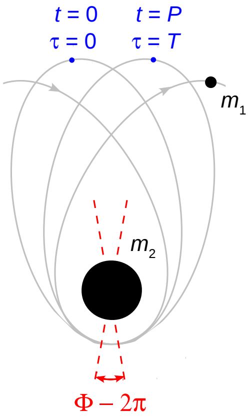

Averaged redshift *vs* semi-latus rectum

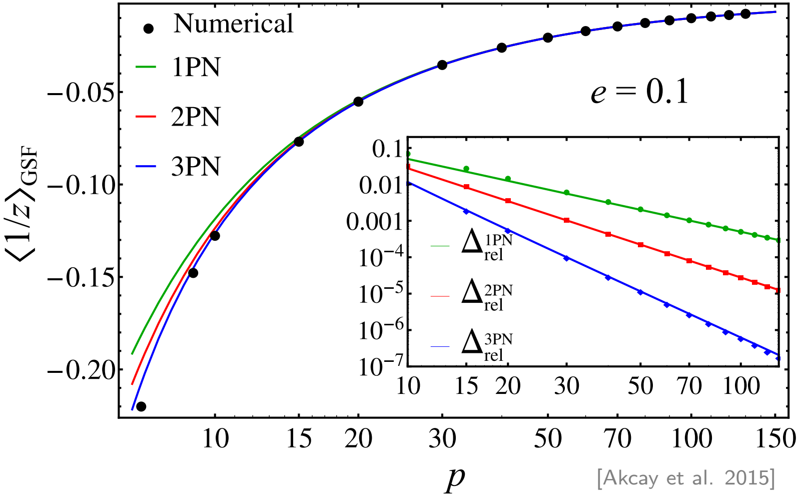

[Akcay et al. 2015]

Averaged redshift *vs* semi-latus rectum

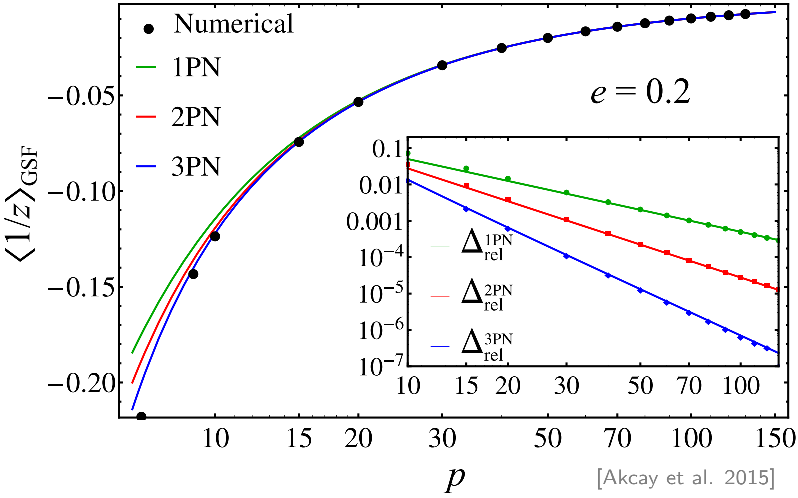

[Akcay et al. 2015]

Averaged redshift *vs* semi-latus rectum

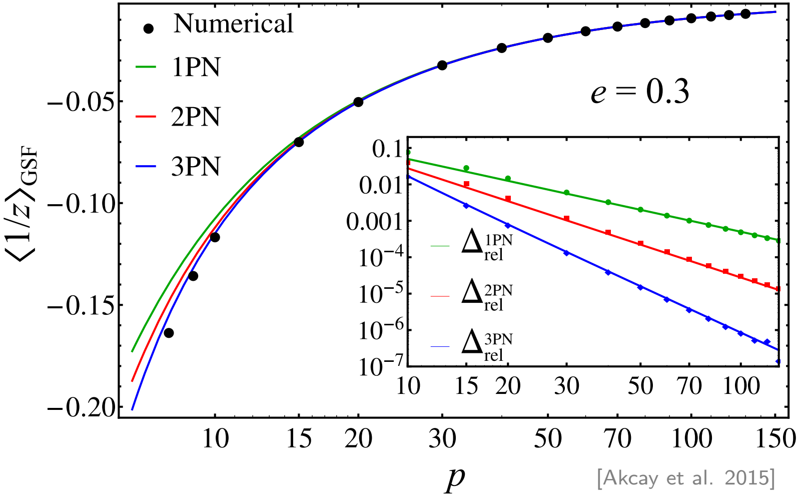

[Akcay et al. 2015]

Averaged redshift *vs* semi-latus rectum

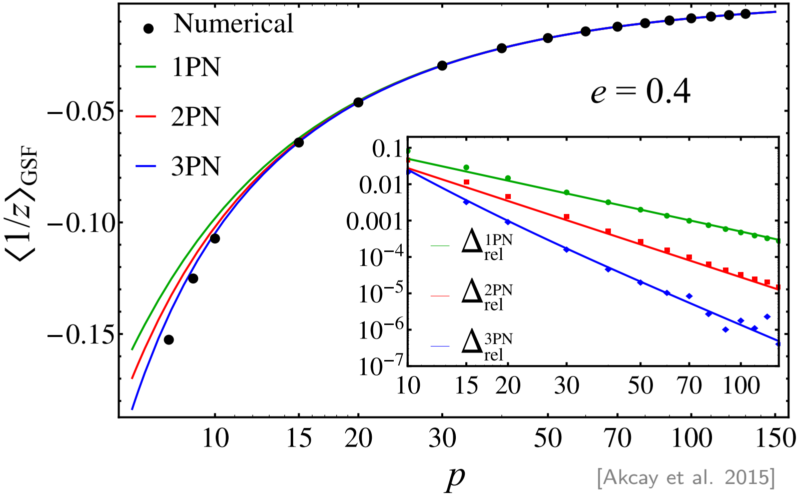

[Akcay et al. 2015]

Extracting post-Newtonian coefficients

	Coeff.	Exact value [Akcay et al. 2015]	Fitted value [Akcay et al. 2015]	Fitted value [Meent, Shah 2015]
	e^2	4	$4.0002(8)$	$4 \pm 6 \times 10^{-12}$
1PN	e^4	-2	$-2.00(1)$	$-2 \pm 4 \times 10^{-10}$
	e^6	0		$0 \pm 4 \times 10^{-9}$

Extracting post-Newtonian coefficients

	Coeff.	Exact value [Akcay et al. 2015]	Fitted value [Akcay et al. 2015]	Fitted value [Meent, Shah 2015]
1PN	e^2	4	$4.0002(8)$	$4 \pm 6 \times 10^{-12}$
	e^4	-2	$-2.00(1)$	$-2 \pm 4 \times 10^{-10}$
	e^6	0		$0 \pm 4 \times 10^{-9}$
2PN	e^2	7	$7.02(2)$	$7 \pm 6 \times 10^{-9}$
	e^4	$1/4$		$1/4 \pm 4 \times 10^{-7}$
	e^6	$5/2$		$5/2 \pm 4 \times 10^{-6}$

Extracting post-Newtonian coefficients

	Coeff.	Exact value [Akcay et al. 2015]	Fitted value [Akcay et al. 2015]	Fitted value [Meent, Shah 2015]
1PN	e^2	4	$4.0002(8)$	$4 \pm 6 \times 10^{-12}$
	e^4	-2	$-2.00(1)$	$-2 \pm 4 \times 10^{-10}$
	e^6	0		$0 \pm 4 \times 10^{-9}$
2PN	e^2	7	$7.02(2)$	$7 \pm 6 \times 10^{-9}$
	e^4	$1/4$		$1/4 \pm 4 \times 10^{-7}$
	e^6	$5/2$		$5/2 \pm 4 \times 10^{-6}$
3PN	e^2	$-14.312097\cdots$	$-14.5(4)$	$-14.3120980(5)$
	e^4	$83.382963\cdots$		$83.38298(7)$
	e^6	$-36.421975\cdots$		$-36.421(3)$

Extracting post-Newtonian coefficients

	Coeff.	Exact value [Akcay et al. 2015]	Fitted value [Akcay et al. 2015]	Fitted value [Meent, Shah 2015]
1PN	e^2	4	$4.0002(8)$	$4 \pm 6 \times 10^{-12}$
	e^4	-2	$-2.00(1)$	$-2 \pm 4 \times 10^{-10}$
	e^6	0		$0 \pm 4 \times 10^{-9}$
2PN	e^2	7	$7.02(2)$	$7 \pm 6 \times 10^{-9}$
	e^4	$1/4$		$1/4 \pm 4 \times 10^{-7}$
	e^6	$5/2$		$5/2 \pm 4 \times 10^{-6}$
3PN	e^2	$-14.312097\cdots$	$-14.5(4)$	$-14.3120980(5)$
	e^4	$83.382963\cdots$		$83.38298(7)$
	e^6	$-36.421975\cdots$		$-36.421(3)$

New coefficients at 4PN and 5PN orders [van de Meent, Shah 2015]

Outline

① Gravitational wave source modelling

② Averaged redshift for eccentric orbits

③ First law of mechanics and applications

First law of binary mechanics

- Canonical ADM Hamiltonian H of two point masses m_a
- Variation δH + Hamilton's equation + orbital averaging:

$$\delta M = \omega\,\delta L + n\,\delta R + \sum_a \langle z_a \rangle\,\delta m_a$$

- First integral associated with the variational first law:

$$M = 2\,(\omega L + nR) + \sum_a \langle z_a \rangle m_a$$

- These relations are satisfied up to *at least* 3PN order

Applications of the first law

- Conservative dynamics beyond the geodesic approximation
- Shift of the Schwarzschild separatrix and singular curve
- Calibration of EOB potentials for generic bound orbits

$$\frac{\partial M}{\partial m_1} = \langle z \rangle - \omega \, \frac{\partial \langle z \rangle}{\partial \omega} - n \, \frac{\partial \langle z \rangle}{\partial n}$$

$$\frac{\partial L}{\partial m_1} = -\frac{\partial \langle z \rangle}{\partial \omega}$$

$$\frac{\partial R}{\partial m_1} = -\frac{\partial \langle z \rangle}{\partial n}$$

Applications of the first law

- Conservative dynamics beyond the geodesic approximation
- Shift of the Schwarzschild **separatrix** and singular curve
- **Calibration of EOB** potentials for generic bound orbits

$$\frac{\partial M}{\partial m_1} = \langle z \rangle - \omega \frac{\partial \langle z \rangle}{\partial \omega} - n \frac{\partial \langle z \rangle}{\partial n}$$

$$\frac{\partial L}{\partial m_1} = -\frac{\partial \langle z \rangle}{\partial \omega}$$

$$\frac{\partial R}{\partial m_1} = -\frac{\partial \langle z \rangle}{\partial n}$$

Schwarzschild separatrix

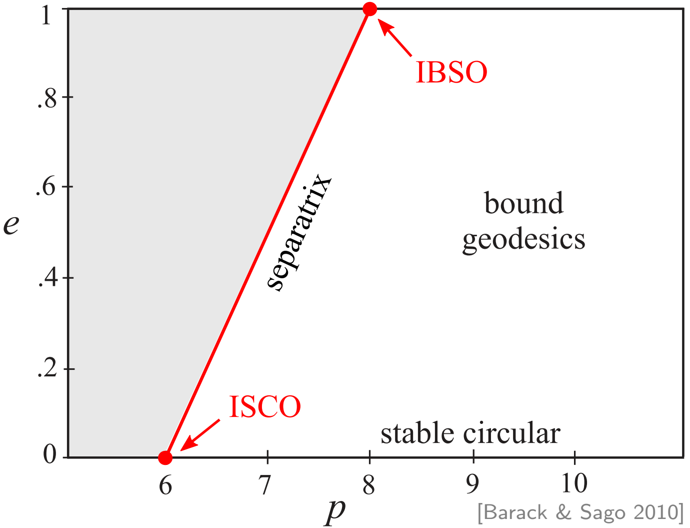

[Barack & Sago 2010]

Schwarzschild separatrix

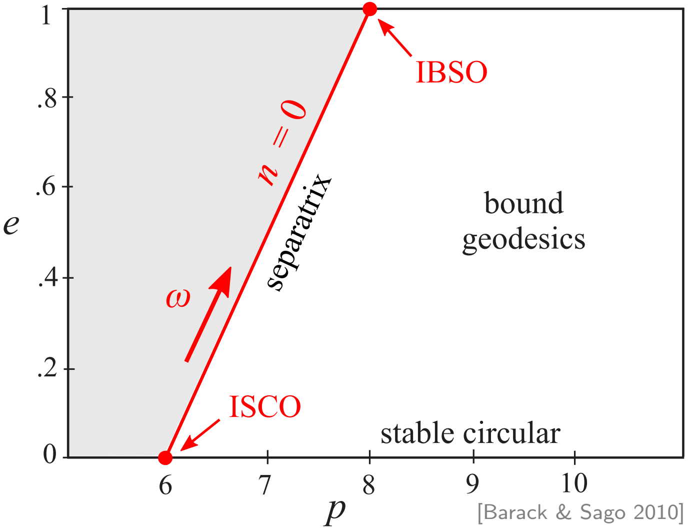

[Barack & Sago 2010]

Shift of the Schwarzschild separatrix

- Separatrix $\omega = \omega_{\text{sep}}(e)$ characterized by the condition

$$n = 0$$

- GSF-induced shift of Schwarzschild ISCO frequency
  [Barack & Sago 2009; Le Tiec et al. 2012; Akcay et al. 2012]

$$\frac{\Delta\omega_{\text{isco}}}{\omega_{\text{isco}}} = 1.2101539(4)\, q$$

- GSF-induced shift of Schwarzschild IBSO frequency ?
- $\mathcal{O}(q)$ shift in $\omega = \omega_{\text{sep}}(e)$ controlled by $\langle z \rangle_{\text{GSF}}(n, \omega)$

EOB dynamics beyond circular motion

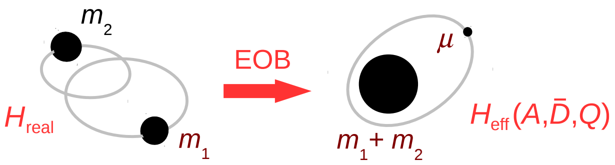

- Conservative EOB dynamics determined by "potentials"

$$A = 1 - 2u + \nu\, a(u) + \mathcal{O}(\nu^2)$$
$$\bar{D} = 1 + \nu\, \bar{d}(u) + \mathcal{O}(\nu^2)$$
$$Q = \nu\, q(u)\, p_r^4 + \mathcal{O}(\nu^2)$$

- Functions $a(u)$, $\bar{d}(u)$ and $q(u)$ controlled by $\langle z \rangle_{\text{GSF}}(n, \omega)$

Summary

- GSF/PN comparison for eccentric orbits relying on $\langle z \rangle(n, \omega)$
- First law of mechanics for eccentric-orbit compact binaries
- Numerous applications of the first law:
  - Conservative dynamics beyond the geodesic approximation
  - Shift of the Schwarzschild separatrix and singular curve
  - Calibration of EOB potentials for generic bound orbits
  - ...

Prospects

- GSF/PN comparison for eccentric orbits relying on $\langle \psi \rangle(n, \omega)$
- Extension of the first law to precessing spinning binaries

Additional Material

Redshift invariant for circular orbits

- It measures the redshift of light emitted from the point particle [Detweiler 2008]

$$\frac{\mathcal{E}_{\rm obs}}{\mathcal{E}_{\rm em}} = \frac{(p^a u_a)_{\rm obs}}{(p^a u_a)_{\rm em}} = z$$

- It is a constant of the motion associated with the helical Killing field k^a:

$$z = -k^a u_a$$

- In coordinates adapted to the symmetry:

$$z = \frac{\mathrm{d}\tau}{\mathrm{d}t} = \frac{1}{u^t}$$

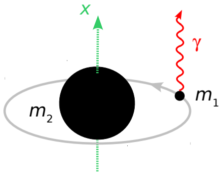

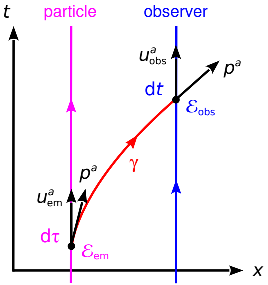

Schwarzschild singular curve

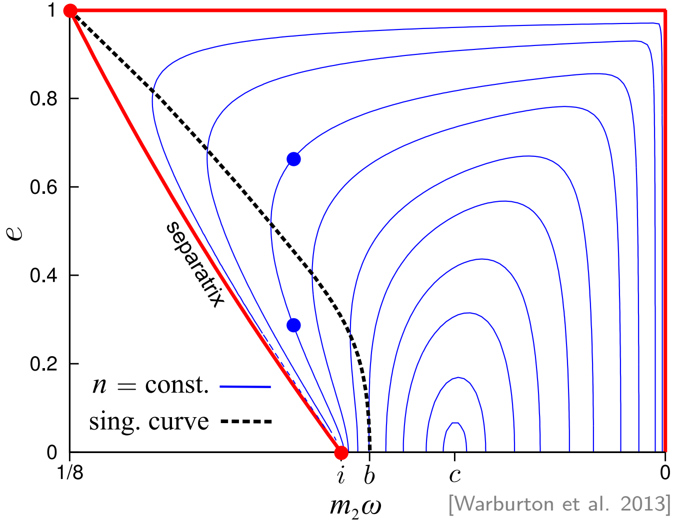

[Warburton et al. 2013]

Schwarzschild singular curve

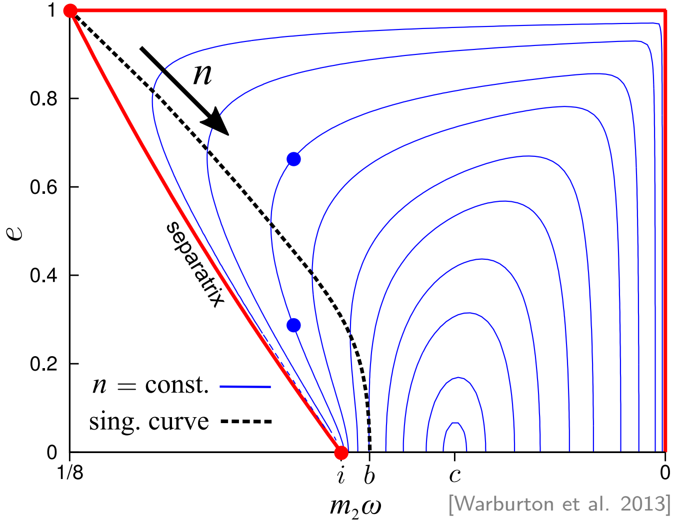

[Warburton et al. 2013]

Shift of the Schwarzschild singular curve

- Singular curve $\omega = \omega_{\text{sing}}(n)$ characterized by condition

$$\left| \frac{\partial(n, \omega)}{\partial(M, L)} \right| = 0$$

- In the test-particle limit $q \to 0$ this is equivalent to

$$\left[\left(\partial^2_{n\omega} \langle z \rangle \right)^2 - \partial^2_n \langle z \rangle \, \partial^2_\omega \langle z \rangle \right]^{-1} = 0$$

- $\mathcal{O}(q)$ shift in $\omega = \omega_{\text{sing}}(n)$ controlled by $\langle z \rangle_{\text{GSF}}(n, \omega)$